# Considerations about Using Polymers in Adaptive Guardrails Construction

**DORIAN NEDELCU[1], GILBERT-RAINER GILLICH[1], FLORENTINA CZIPLE [1], ION CIUCĂ[2], ION PĂDUREAN[3]**

[1] Eftimie Murgu University of Re°iþa, 1-4 P-ta Traian Vuia, 320085 Resita, Romania

[2] Politehnica University of Bucharest, 313 Splaiul Independentei, 060021, Bucuresti, România

[3] Politehnica University of Timisoara, 1 Bd. M. Viteazul, 300222, Timisoara, Romania

*Guardrails are systems designed to keep vehicles in certain places, by preventing access in dangerous areas. They can be a source of injuries because their rigid structure, designed to face high level of strength. Depending on their speed and mass, vehicles can load guardrails in various forms. The authors propose the use of adaptive guardrails, involving polymers, which react different by different load levels. The behaviour is studied using modeling and simulation with the FEM; different types of guardrails and external loads displacement and stress are presented, as support to choose the most convenient type of guardrail for each application.*

*Keywords: adaptive guardrails, traffic security, polymers, FEM simulation*

A guardrail is a system designed to keep vehicles in certain places, avoiding unintentionally straying into dangerous or off-limits areas. Placed along roads, guardrails prevent vehicles from veering into oncoming traffic, crashing against solid objects or falling into ravines. In industrial plans, guardrails have the role to prevent vehicles to enter or cross dangerous areas or to crash against build structures or machines. Guardrails are also frequently placed beneath the sides of high-sided heavy trucks or trailers, in order to prevent smaller vehicles like cars or motorcycles or people from passing under the heavier vehicle during a collision and being crushed by its back wheels.

Usually guardrails are made of a rigid metallic structure, (fig. 1), using a metallic horizontal band (in most cases a W profile) that transfers the impact force to multiple vertical supports to which it is connected. In some applications the horizontal band is fixed on constructions or special concrete elements. They are able to stop the movement of vehicles in unwanted directions, sometimes deflecting the vehicle back in the traffic (particularly dangerous on undivided roadways, as the vehicle may travel into oncoming traffic), but are the source of numerous injuries [1, 2].

Collapsible guardrails are safer than rigid ones, since longer collision duration will result in a smaller average impact force. This may be achieved by designing the supports so that they break off on impact, allowing the barrier to deform and absorb energy. In any case the vehicles crushing a classical guardrail will be damaged, irrespective their speed.

The authors propose the use of adaptive guardrails, which react different for different impact forces, aiming to diminish damages on vehicles. The guardrails are realized of metal and talc-reinforced high density polyethylene (HDPE) or polypropylene copolymer (COPP). In the first step, for very low speed, the polymeric protection element of the guardrail overtakes the load, getting elastic deformation. Based on the fact that talc avoids the appearance of abrasive particles in the polymers [3, 7], the paint of the vehicle by scrubbing will be protected. This case is frequently met in garages or narrow places, where speed is drastically reduced.

By higher speed the polymeric protection element gets his maximum deformation and the impact force is transmitted to the special band and her fixing system, which absorbs energy trough displacement and deformation. The polymeric protection element being in this case pressed on the band will maintain its integrity, together with the band. It has to be mentioned that polymers allow numerous flexures [3, 7, 8], so that the collapse of the protection element is avoided. The fixing system is responsible for the impact energy absorption, by permitting a displacement of the band until a limit position,

Fig. 1. Guardrail placed along roads

* *email: d.nedelcu@uem.ro*

**Table 1**
PHYSICAL AND MECHANICAL PROPERTIES OF THE CHOSEN POLYMERS

| Material | Unit | Salflex 525T | Salflex 620TIM | Salflex 620TIC | Test method | PP Copolymer | Alloy Steel |
|---|---|---|---|---|---|---|---|
| Density | g/cm$^3$ | 1,14 | 1,03 | 1,04 | ISO 1183 | 0.89 | 7.7 |
| Poisson's ratio | - | 0,395 | 0,387 | 0,385 | ISO 527 | 0.41 | 0.28 |
| Tensile Stress at Yield | MPa | 25 | 20 | 21 | ISO 527 -1, -2 | - | 620.4 |
| Tensile Strain at Break | % | - | 60 | 4 | ISO 527 -1, -2 | - | - |
| Elastic Modulus | MPa | 2400 | 1900 | 2170 | ISO 178 | 896 | 210000 |
| Noched Izod Impact strength (23°) | kJ/m$^2$ | 20,0 | 21,0 | 19,1 | ISO 180 | - | - |

where the band is blocked to avoid the deflection of vehicles back in the traffic. By deactivating the blocking system the band will take its initial position, so no damages on the guardrail and limited damages on the vehicle will take place.

The third action that an adaptive guardrail will take, for high speed of vehicles, is the collapse of the support elements, by maintaining the integrity of the band. This prevents vehicles from accessing dangerous areas or crashing against objects or persons.

Therefore results the need to study the behaviour of the polymeric protection element using numerical modeling and simulation, for different involved materials and constructive types. This study continue the researches done by some authors using instrumental and computational support [4, 5, 9, 10], regarding the behaviour of polymers in industrial applications.

## Experimental part

Materials proposed to be involved as polymeric protection elements are products of Salflex Polymers Ltd., destined for automotive and industrial applications, with the main physical and mechanical properties presented in table 1. For results comparison, were considered also the following materials: the polymer PP Copolymer and the Alloy Steel, with properties taken from database of the Cosmos Design Star finite element software.

They are talc-reinforced polymers, the talc filer being 25% for Salflex 525T and 20% for Salflex 620TIM respectively Salflex 620TC. The use of talc, $Mg_3Si_4O_{10}(OH)_2$, is righteous based on characteristics which it transmit to polymers [4, 7, 8]; it increases mechanical properties, avoids creation of abrasive particles and increases the resistance against water vapors. Because the results for the three materials conduct to similar results, differences been evidenced just in the values of the displacement (for the other two materials they are smaller with 10…15%), we took in consideration in this paper just Salflex 525T.

Regarding the constructive types, we have analysed protection elements with the length $L$=1000 mm, for parameters thickness $g$=4, 5, 6 mm and width spire h=20, 26, 30 mm (fig. 2).

Numerical simulation was made with Cosmos Design Star, a powerful finite element software [6]. The following elements are required for numerical simulation:

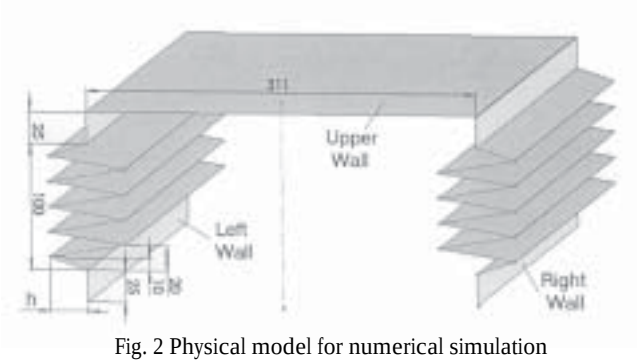

Fig. 2 Physical model for numerical simulation

- the model geometry: the section geometry was sketched in Design Star, figure 2 and the length of the guardrail was generated as a surface by extrusion; the parameters thickness "g" and width spire "h" was involved in this study;
- the material properties: Elastic Modulus and Poisson's ratio are defined in table 1;
- the mesh of the model, was generated by Design Star, figure 3;
- loads and restraints schema: the restraints applied to the model prevent the motion (fig. 3).

Theoretically it is possible to mesh any solid model with tetrahedral solid elements. However, meshing thin models with solid elements results in generating a large number of elements since it is necessary to use a small element

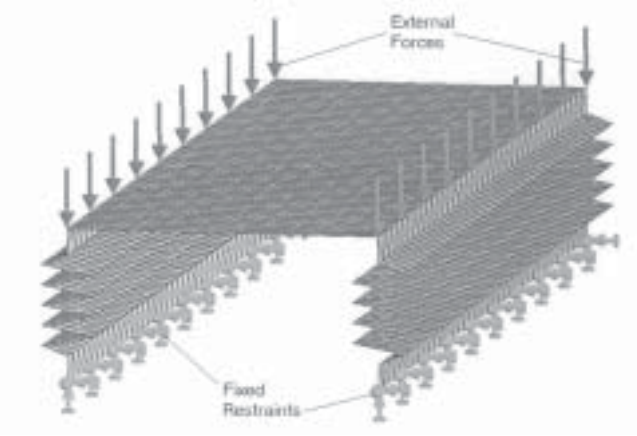

Fig. 3 Loads and restraints schema

size. Using a larger element size deteriorates the quality of the mesh and leads to inaccurate results [9]. Shell meshing is the natural choice for sheet metal and thin parts. Surface models can only be meshed with shell elements (triangular elements). For a shell study, it is possible to select one of two options:

- draft quality mesh: the automatic mesher generates linear triangular shell elements, defined by 3 corner nodes connected by 3 straight edges;
- high quality mesh: the automatic mesher generates parabolic triangular shell elements, defined by 3 corner nodes, 3 mid-side nodes, and 3 parabolic edges; this mesh was used in the present study, figure 3.

Every shell node has 6 degrees of freedom, which are the translations and rotations for the three orthogonal axes. Every shell has one top face and one bottom face, which must be aligned, because the results are in general not identically on the two faces.

Figure 3 presents the restraints and load scheme. The left and right walls are fixed at the bottom edge. For shell meshes, fixed restraints set the translational and the rotational degrees of freedom to zero. The external forces are applied to the left and right wall upper edge.

**Table 2**

NUMERICAL RESULTS FOR PARAMETER h=20 mm

| Input Parameters | | Units | Set 1 | Set 2 | Set 3 | Set 4 | Set 5 | Set 6 |
|---|---|---|---|---|---|---|---|---|
| Force | | N | 14500 | 10000 | 8000 | 6000 | 3000 | 2000 |
| Thickness | Material | Salflex 525T | | | | | | |
| 6 | Stress von Mises | MPa | 15.04 | 10.37 | 8.30 | 6.22 | 3.11 | 2.07 |
| | Resultant displacement | mm | 6.18 | 4.26 | 3.41 | 2.56 | 1.28 | 0.85 |
| 5 | Stress von Mises | MPa | 19.67 | 13.56 | 10.85 | 8.14 | 4.07 | 2.71 |
| | Resultant displacement | mm | 9.42 | 6.50 | 5.20 | 3.90 | 1.95 | 1.30 |
| 4 | Stress von Mises | MPa | 27.25 | 18.79 | 15.03 | 11.28 | 5.64 | 3.76 |
| | Resultant displacement | mm | 16.01 | 11.04 | 8.84 | 6.63 | 3.31 | 2.21 |
| Thickness | Material | Salflex 620TIM | | | | | | |
| 6 | Stress von Mises | MPa | 15.08 | 10.40 | 8.32 | 6.24 | 3.12 | 2.08 |
| | Resultant displacement | mm | 7.82 | 5.39 | 4.32 | 3.24 | 1.62 | 1.08 |
| 5 | Stress von Mises | MPa | 19.71 | 13.59 | 10.87 | 8.15 | 4.08 | 2.72 |
| | Resultant displacement | mm | 11.92 | 8.22 | 6.58 | 4.93 | 2.47 | 1.64 |
| 4 | Stress von Mises | MPa | 27.32 | 18.84 | 15.07 | 11.30 | 5.65 | 3.77 |
| | Resultant displacement | mm | 20.26 | 13.97 | 11.18 | 8.38 | 4.19 | 2.79 |
| Thickness | Material | Salflex 620TIC | | | | | | |
| 6 | Stress von Mises | MPa | 15.09 | 10.41 | 8.32 | 6.24 | 3.12 | 2.08 |
| | Resultant displacement | mm | 6.85 | 4.73 | 3.78 | 2.84 | 1.42 | 0.95 |
| 5 | Stress von Mises | MPa | 19.72 | 13.60 | 10.88 | 8.16 | 4.08 | 2.72 |
| | Resultant displacement | mm | 10.45 | 7.20 | 5.76 | 4.32 | 2.16 | 1.44 |
| 4 | Stress von Mises | MPa | 27.33 | 18.85 | 15.08 | 11.31 | 5.66 | 3.77 |
| | Resultant displacement | mm | 17.75 | 12.24 | 9.79 | 7.34 | 3.67 | 2.45 |
| Thickness | Material | PP Copolymer | | | | | | |
| 6 | Stress von Mises | MPa | 14.92 | 10.29 | 8.23 | 6.17 | 3.09 | 2.06 |
| | Resultant displacement | mm | 16.46 | 11.35 | 9.08 | 6.81 | 3.41 | 2.27 |
| 5 | Stress von Mises | MPa | 19.57 | 13.50 | 10.80 | 8.10 | 4.05 | 2.70 |
| | Resultant displacement | mm | 25.13 | 17.33 | 13.86 | 10.40 | 5.20 | 3.47 |
| 4 | Stress von Mises | MPa | 27.14 | 18.71 | 14.97 | 11.23 | 5.61 | 3.74 |
| | Resultant displacement | mm | 42.75 | 29.48 | 23.58 | 17.69 | 8.84 | 5.90 |
| Thickness | Material | Alloy Steel | | | | | | |
| 6 | Stress von Mises | MPa | 15.62 | 10.77 | 8.62 | 6.46 | 3.23 | 2.15 |
| | Resultant displacement | mm | 0.07 | 0.05 | 0.04 | 0.03 | 0.01 | 0.01 |
| 5 | Stress von Mises | MPa | 20.36 | 14.04 | 11.23 | 8.42 | 4.21 | 2.81 |
| | Resultant displacement | mm | 0.11 | 0.08 | 0.06 | 0.05 | 0.02 | 0.02 |
| 4 | Stress von Mises | MPa | 28.26 | 19.49 | 15.59 | 11.70 | 5.85 | 3.90 |
| | Resultant displacement | mm | 0.19 | 0.13 | 0.10 | 0.08 | 0.04 | 0.03 |

**Table 3**

NUMERICAL RESULTS FOR PARAMETER h=26 mm

| Input Parameters | | Units | Set 1 | Set 2 | Set 3 | Set 4 | Set 5 | Set 6 |
|---|---|---|---|---|---|---|---|---|
| Force | | N | 14500 | 10000 | 8000 | 6000 | 3000 | 2000 |
| Thickness | Material | Salflex 525T | | | | | | |
| 6 | Stress von Mises | MPa | 25.95 | 17.90 | 14.32 | 10.74 | 5.37 | 3.58 |
| | Resultant displacement | mm | 16.24 | 11.20 | 8.96 | 6.72 | 3.36 | 2.24 |
| 5 | Stress von Mises | MPa | 36.18 | 24.95 | 19.96 | 14.97 | 7.49 | 4.99 |
| | Resultant displacement | mm | 27.21 | 18.77 | 15.01 | 11.26 | 5.63 | 3.75 |
| 4 | Stress von Mises | MPa | 54.01 | 37.25 | 29.80 | 22.35 | 11.18 | 7.45 |
| | Resultant displacement | mm | 51.40 | 35.45 | 28.36 | 21.27 | 10.63 | 7.09 |
| Thickness | Material | Salflex 620TIM | | | | | | |
| 6 | Stress von Mises | MPa | 25.95 | 17.89 | 14.32 | 10.74 | 5.37 | 3.58 |
| | Resultant displacement | mm | 20.63 | 14.23 | 11.38 | 8.54 | 4.27 | 2.85 |
| 5 | Stress von Mises | MPa | 36.17 | 24.94 | 19.95 | 14.97 | 7.48 | 4.99 |
| | Resultant displacement | mm | 34.58 | 23.85 | 19.08 | 14.31 | 7.15 | 4.77 |
| 4 | Stress von Mises | MPa | 53.97 | 37.22 | 29.78 | 22.33 | 11.17 | 7.44 |

contnuare

| | | | | | | | | |
|---|---|---|---|---|---|---|---|---|
| | Resultant displacement | mm | 65.32 | 45.05 | 36.04 | 27.03 | 13.51 | 9.01 |
| Thickness | Material | | Salflex 620TIC | | | | | |
| 6 | Stress von Mises | MPa | 25.94 | 17.89 | 14.31 | 10.74 | 5.37 | 3.58 |
| | Resultant displacement | mm | 18.09 | 12.48 | 9.98 | 7.49 | 3.74 | 2.50 |
| 5 | Stress von Mises | MPa | 36.16 | 24.94 | 19.95 | 14.96 | 7.48 | 4.99 |
| | Resultant displacement | mm | 30.32 | 20.91 | 16.73 | 12.55 | 6.27 | 4.18 |
| 4 | Stress von Mises | MPa | 53.96 | 37.22 | 29.77 | 22.33 | 11.16 | 7.44 |
| | Resultant displacement | mm | 57.28 | 39.50 | 31.60 | 23.70 | 11.85 | 7.90 |
| Thickness | Material | | PP Copolymer | | | | | |
| 6 | Stress von Mises | MPa | 25.98 | 17.91 | 14.33 | 10.75 | 5.37 | 3.58 |
| | Resultant displacement | mm | 42.98 | 29.64 | 23.71 | 17.78 | 8.89 | 5.93 |
| 5 | Stress von Mises | MPa | 36.23 | 24.99 | 19.99 | 14.99 | 7.50 | 5.00 |
| | Resultant displacement | mm | 72.02 | 49.67 | 39.74 | 29.80 | 14.90 | 9.93 |
| 4 | Stress von Mises | MPa | 54.11 | 37.32 | 29.85 | 22.39 | 11.20 | 7.46 |
| | Resultant displacement | mm | 136.0 | 93.80 | 75.04 | 56.28 | 28.14 | 18.76 |
| Thickness | Material | | Alloy Steel | | | | | |
| 6 | Stress von Mises | MPa | 26.12 | 18.01 | 14.41 | 10.81 | 5.40 | 3.60 |
| | Resultant displacement | mm | 0.20 | 0.14 | 0.11 | 0.08 | 0.04 | 0.03 |
| 5 | Stress von Mises | MPa | 36.30 | 25.03 | 20.03 | 15.02 | 7.51 | 5.01 |
| | Resultant displacement | mm | 0.33 | 0.23 | 0.18 | 0.14 | 0.07 | 0.05 |
| 4 | Stress von Mises | MPa | 54.01 | 37.25 | 29.80 | 22.35 | 11.18 | 7.45 |
| | Resultant displacement | mm | 0.63 | 0.43 | 0.35 | 0.26 | 0.13 | 0.09 |

**Table 4**

NUMERICAL RESULTS FOR PARAMETER h=30 mm

| Input Parameters | | Units | Set1 | Set2 | Set3 | Set4 | Set5 | Set6 |
|---|---|---|---|---|---|---|---|---|
| Force | | N | 14500 | 10000 | 8000 | 6000 | 3000 | 2000 |
| Thickness | Material | | Salflex 525T | | | | | |
| 6 | Stress von Mises | MPa | 28.99 | 19.99 | 16.00 | 12.00 | 6.00 | 4.00 |
| | Resultant displacement | mm | 24.25 | 16.73 | 13.38 | 10.04 | 5.02 | 3.35 |
| 5 | Stress von Mises | MPa | 40.64 | 28.03 | 22.42 | 16.82 | 8.41 | 5.61 |
| | Resultant displacement | mm | 40.89 | 28.20 | 22.56 | 16.92 | 8.46 | 5.64 |
| 4 | Stress von Mises | MPa | 63.65 | 43.89 | 35.12 | 26.34 | 13.17 | 8.78 |
| | Resultant displacement | mm | 77.89 | 53.72 | 42.98 | 32.23 | 16.12 | 10.74 |
| Thickness | Material | | Salflex 620TIM | | | | | |
| 6 | Stress von Mises | MPa | 30.06 | 20.73 | 16.59 | 12.44 | 6.22 | 4.15 |
| | Resultant displacement | mm | 30.83 | 21.26 | 17.01 | 12.76 | 6.38 | 4.25 |
| 5 | Stress von Mises | MPa | 42.10 | 29.03 | 23.23 | 17.42 | 8.71 | 5.81 |
| | Resultant displacement | mm | 51.97 | 35.84 | 28.67 | 21.50 | 10.75 | 7.17 |
| 4 | Stress von Mises | MPa | 63.62 | 43.87 | 35.10 | 26.33 | 13.16 | 8.77 |
| | Resultant displacement | mm | 99.01 | 68.28 | 54.63 | 40.97 | 20.49 | 13.66 |
| Thickness | Material | | Salflex 620TIC | | | | | |
| 6 | Stress von Mises | MPa | 30.06 | 20.73 | 16.58 | 12.44 | 6.22 | 4.15 |
| | Resultant displacement | mm | 27.03 | 18.64 | 14.92 | 11.19 | 5.59 | 3.73 |
| 5 | Stress von Mises | MPa | 42.10 | 29.03 | 23.23 | 17.42 | 8.71 | 5.81 |
| | Resultant displacement | mm | 45.57 | 31.43 | 25.14 | 18.86 | 9.43 | 6.29 |
| 4 | Stress von Mises | MPa | 63.61 | 43.87 | 35.10 | 26.32 | 13.16 | 8.77 |
| | Resultant displacement | mm | 86.83 | 59.88 | 47.90 | 35.93 | 17.96 | 11.98 |
| Thickness | Material | | PP Copolymer | | | | | |
| 6 | Stress von Mises | MPa | 29.01 | 20.01 | 16.01 | 12.00 | 6.00 | 4.00 |
| | Resultant displacement | mm | 64.18 | 44.26 | 35.41 | 26.56 | 13.28 | 8.85 |
| 5 | Stress von Mises | MPa | 42.15 | 29.07 | 23.26 | 17.44 | 8.72 | 5.81 |
| | Resultant displacement | mm | 108.1 | 74.60 | 59.68 | 44.76 | 22.38 | 14.92 |
| 4 | Stress von Mises | MPa | 63.71 | 43.94 | 35.15 | 26.36 | 13.18 | 8.79 |
| | Resultant displacement | mm | 206.0 | 142.1 | 113.6 | 85.26 | 42.63 | 28.42 |
| Thickness | Material | | Alloy Steel | | | | | |
| 6 | Stress von Mises | MPa | 29.23 | 20.16 | 16.13 | 12.10 | 6.05 | 4.03 |
| | Resultant displacement | mm | 0.30 | 0.21 | 0.16 | 0.12 | 0.06 | 0.04 |
| 5 | Stress von Mises | MPa | 42.34 | 29.20 | 23.36 | 17.52 | 8.76 | 5.84 |
| | Resultant displacement | mm | 0.50 | 0.35 | 0.28 | 0.21 | 0.10 | 0.07 |
| 4 | Stress von Mises | MPa | 63.89 | 44.06 | 35.25 | 26.44 | 13.22 | 8.81 |
| | Resultant displacement | mm | 0.96 | 0.66 | 0.53 | 0.40 | 0.20 | 0.13 |

## Results and discussions

For the guardrail's polymeric protection element were imposed three thickness values: 4, 5, 6 mm and width spire h=20, 26, 30 mm, for a domain loading values between 2000 and 14500 N. The maximal value corresponds to a standard car moving with low speed. The results are presented in table 2, 3 and 4.

In table 2-4 the displacement represents the resultant displacement between the X, Y and Z components of the

displacement direction, and von Mises stress is a scalar quantity calculated from stress components, with no direction and fully defined by magnitude with stress units. The von Mises stress is used by failure criteria and is computed from the following six components:

$$\sigma_{VonMises} = \sqrt{\frac{1}{2}\left[(\sigma_X - \sigma_Y)^2 + (\sigma_X - \sigma_Z)^2 + (\sigma_Y - \sigma_Z)^2\right] + 3\left[\tau_{XY}{}^2 + \tau_{XZ}{}^2 + \tau_{YZ}{}^2\right]} \quad (1)$$

where: $\sigma_X$, $\sigma_Y$, $\sigma_Z$ are normal stresses in X, Y, Z direction and $\tau_{XY}$, $\tau_{XZ}$, $\tau_{YZ}$ are shears in Y direction on YZ plane, Z direction on YZ plane and Z direction on XZ plane respectively.

The main purpose of the study was to obtain maximal displacements of the adaptive guardrail, by maintaining the stress under 20 MPa, value which corresponds to tensile stress at yield for Salflex polymers. Because numerical simulation was made for elastic domain, with respect of the Hook law, the values resulted form simulation over 20 MPa will not be considered, being marked with gray color in the tables 2, 3 and 4.

The regions with highest level of von Mises stress, with values presented in table 2 - 4 are situated at the extremities of the triangles (fig. 4). The maximal values of displacement are localized at the upper wall, decreasing until zero to the edge where fixed restraints were applied.

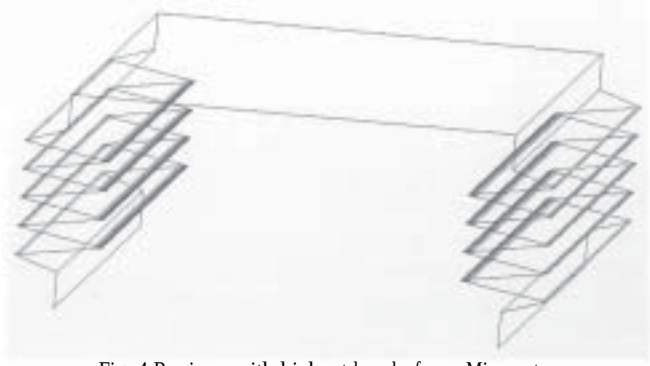

Fig. 4 Regions with highest level of von Mises stress

The figures 5, 6, and 7 present the variations of the Force – Material/Thickness – Stress von Mises for values 20, 26, 30 of the "h" parameter.

The figures 8, 9, and 10 present the variations of the Force – Material/Thickness – Displacement for values 20, 26, 30 of the "h" parameter.

From the tables 2,-4 and figures 5-10, the following conclusions results:

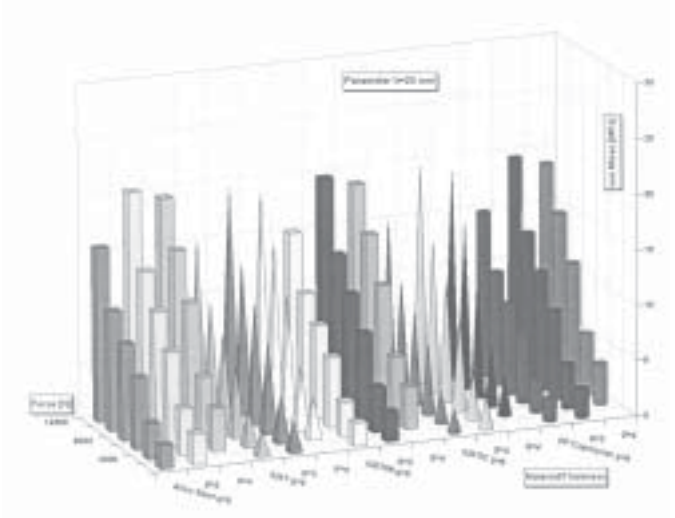

Fig. 5 The variations of the Force – Material/Thickness – Stress von Mises for values h=20 mm

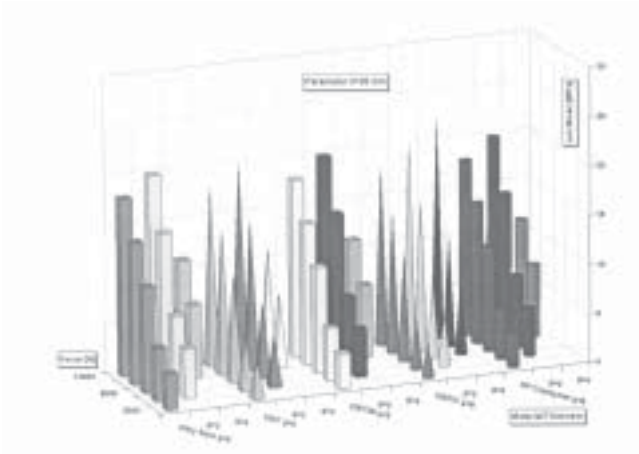

Fig. 6 The variations of the Force – Material/Thickness – Stress von Mises for values h=26 mm

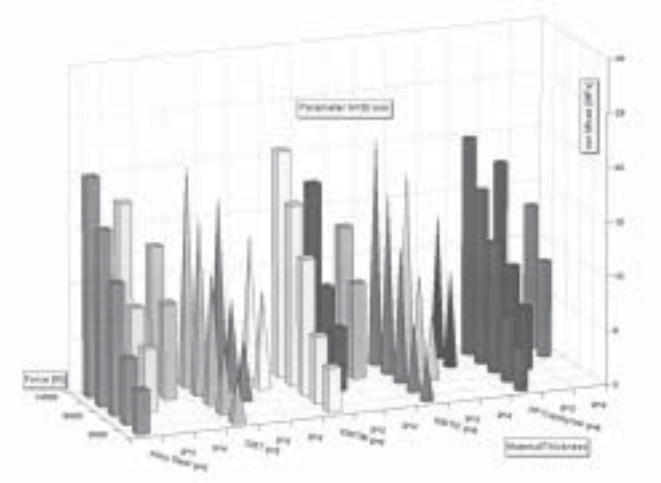

Fig. 7 The variations of the Force – Material/Thickness – Stress von Mises for values h=30 mm

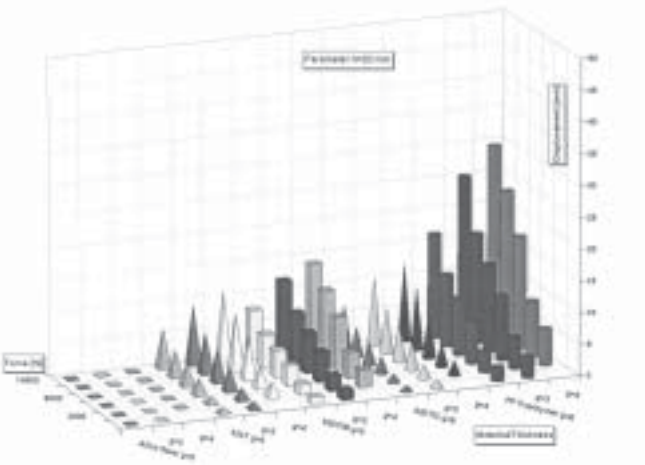

Fig. 8 The variations of the Force – Material/Thickness – Displacement for values h=20 mm

- for the same value of width spire "h" and thickness "g", the influence of the material properties over the stress von Mises is more reduced comparative with the deformation influence, and the Elastic Modulus has a significance influence than Poisson's ratio; the deformations rise when Elastic Modulus decrease; so, for Alloy Steel, with the highest value of Elastic Modulus, the deformations are the smallest, in the domain 0.01…0.21; the highest deformation values are obtained in the domain 2.27...44.76 for PP Copolymer material, with the lowest

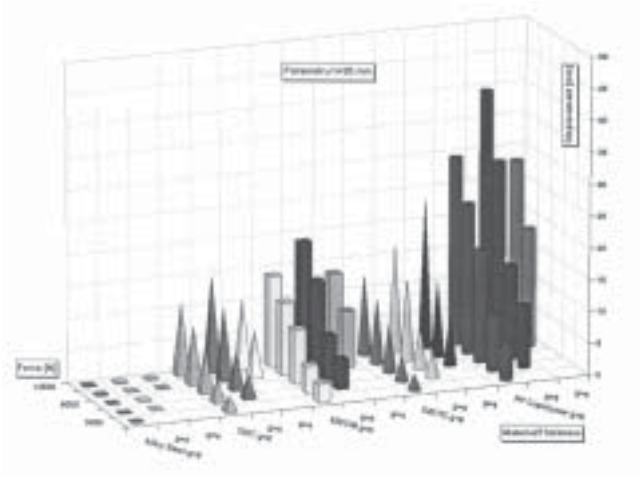

Fig. 9 The variations of the Force – Material/Thickness – Displacement for values h=26 mm

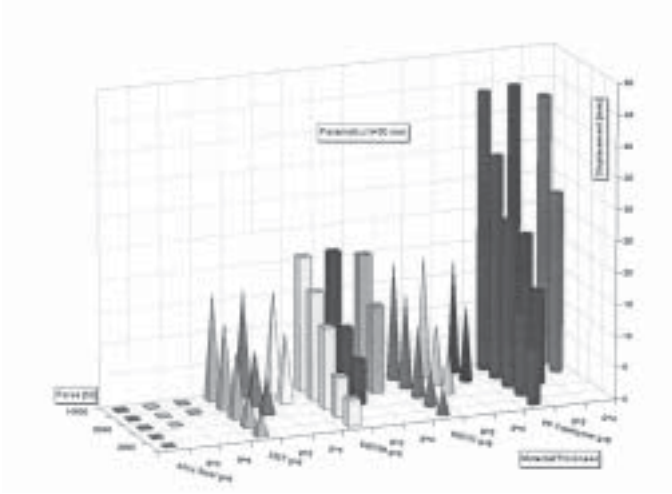

Fig. 10 The variations of the Force – Material/Thickness – Displacement for values h=30 mm

value for Elastic Modulus; for Salflex materials, with intermediate values, but quite close, are obtained deformation values in domain 0.85…23.7 mm;

- for the same value of the width spire "h", the deformation and stress von Mises rise with thickness "g" decrease;

- for the same value of the thickness "g" the deformation and stress von Mises rise with width spire "h" increase.

## Conclusions

The calculated variations permit to select the optimal values parameters (thickness "g" and width spire "h") of the polymeric protection element for possible loads and materials. So, for the admitted stress values, it is possible to select the proper dimensions, to obtain the contact between the upper wall and the metallic band, which will support further the loads. To obtain the main function of the adaptive guardrail (maximal deformation) must be selected a polymeric material with a reduced value for Elastic Modulus.

A **s**imple shape of the polymeric protection element assures a supplementary protection for vehicles and people, avoiding injury and damages, because of the deformation and energy absorbing processes generated.

The following researches will be focus on shapes with variable thickness, with higher values for the most stressed regions.

## References


1. McDEVITT. C., Basics of Concrete Barriers, Public Roads, **63**, nr. 5, 2000 p. 217

2. SZE, N.N., WONG, S.C., Diagnostic analysis of the logistic model for pedestrian injury severity in traffic crashes, Accident Analysis and Prevention, **39**, 2007, p. 1267

3. GILLICH, G.R., SAMOILESCU, G., BERINDE, F.C., CHIONCEL, C.P., Determinarea experimentalã a caracteristicii de rigiditate ºi a modulului de elasticitate a cauciucului utilizând reprezentarea timp-frecvenþã, Mat. Plast., **44**, nr. 1, 2007, p. 18

4. VODÃ, M., BORDEA ªU, I., MESMACQUE, G., CHIÞAC, V., TABÃRA, I., Aspecte ale comportamentului asamblãrilor din polimeri la solicitãri mecanice, Mat. Plast., **44**, nr. 3, 2007, p. 254

5. GHITA, E., GILLICH, G.R., BORDEA ªU, I., VODÃ, M., TROI, C., Aspecte ale comportãrii polimerilor la solicitãri de tracþiune, Mat. Plast., **44**, nr. 2, 2007, p. 158

6. MĂNESCU, T., NEDELCU, D., Analizã structuralã prin metoda elementului finit, Editura "Orizonturi Universitare", ISBN 973-638-217-6, Timiºoara 2005, p. 11

7. GHIOCA, P., BUZDUGAN, E., CINCU, C., IANCU LORENA., ZAHARIA, C., ZECHERU, TEODORA.,Compozite politeilenice antisoc, Mat.Plast., **44**, nr.3, 2007, p.175

8. PAUN V., P., An Estimation, of the Polymer Translocation Time through membrane, Mat.Plast, **43**, 1, 2006, p.51

9. HADAR, A., BORDEASU I., MITELEA I.. VLASCEANU D., Validarea experimentala a unui model teoretic folosit in calculul de rezistenta al structurilor realizate din materiale compozite, Mat. Plast, **43**, 1, 2006, p.70

10. PAPANICOLAU, G., JIGA, G., GIANNIS S.P., Residual Tensile Strength after Impact of Woven Glass/Polyester reinforced Composites, Mat.Plast. **44**, 3, 2007, p.250



Manuscript received: 14.11.2007